Near-surface wind and wave drift currents in the coupled air-sea boundary layer

R. M. Samelson - CEOAS, Oregon State University, Corvallis OR USA - roger.samelson@oregonstate.edu

Abstract: This project will use a combination of theoretical, numerical, and satellite and in-situ data analysis to improve understanding of wind-drift and wave-drift currents in the upper few meters of the water column and their coupling across the air-sea interface to the atmospheric boundary layer. The proposed effort extends and is motivated by recent research results (Samelson 2022) that offer a new approach to representing and understanding the dynamics of the wind and wave driven components of near-surface currents and their role in the coupled air-sea boundary layer. The mean momentum balance is formulated in terms of a mass-weighted spatial average in surface-conforming coordinates that captures the total mean parcel motion. The resulting equilibrium wind-drift model incorporates a novel, wind-speed-dependent wave-effect parameter, which allows wave effects on momentum transport that cause departures from rigid-wall boundary layer structure to be consistently represented within the mean dynamics. The project activities will focus on three elements that are relevant to planning for a future Doppler scatterometer winds and currents mission: (a) characterization and analysis of the global (extra-equatorial) properties of sub-inertial wind-drift currents predicted by the new equilibrium wind-drift model and their implications for the associated Doppler scatterometer sampling problem; (b) examination of the role of sub-inertial wind-drift currents in ocean-atmosphere interaction in coupled numerical simulations of the northern California Current System; and (c) assessment and refinement of the new equilibrium wind-drift model through comparison with existing near-surface current observations.

Samelson, R. M., 2022. Wind drift in a homogeneous equilibrium sea. J. Phys. Oceanogr., 52, 1945-1967. doi: 10.1175/JPO-D-22-0017.1.

1. Capturing Stokes drift in Eulerian means

The mean momentum balance is formulated in terms of a mass-weighted Eulerian spatial average in surface-conforming coordinates. This average captures the total mean parcel motion. For a linear sinusoidal wave, for example, the mean wave momentum is represented in different ways, depending on the averaging method that is used (Figure 1). **For a fixed-depth Eulerian average, the mean momentum is zero below the wave trough level, and all the mean momentum is placed between the trough and crest levels (Fig. 1, green line).** For a parcel-following Lagrangian mean, the mean momentum appears in the exponentially decaying Stokes-drift profile (Fig. 1, blue line). The total depth-integrated mean wave momentum is the same for the fixed-depth Eulerian and parcel-following Stokes-drift averages. **For the mass-weighted Eulerian spatial average in surface-conforming coordinates, the mean momentum appears in an exponentially decaying profile that has the same form and amplitude as the Stokes-drift profile (Fig. 1, blue line).**

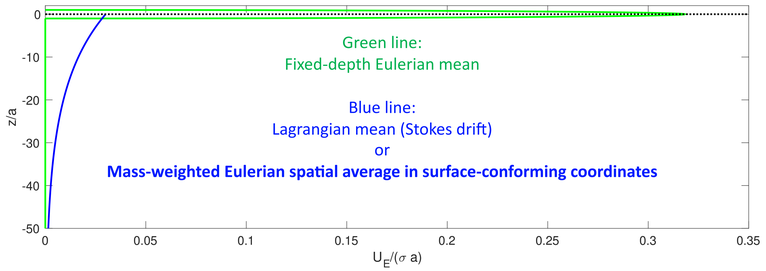

Figure 1: Dimensionless mean velocity vs. dimensionless depth for a linear sinusoidal wave with frequency σ, wavenumber k, and free-surface displacement amplitude a, for wave steepness *k*a = 0.03.

2. Model for equilibrium wind and wave drift: formulation

The mass-weighted mean horizontal momentum balance for the ageostrophic flow in a homogeneous, equilibrium sea is classical in appearance:

$$\rho_o f\,\mathbf{k}\times\mathbf{U} = -\frac{d\tau}{dz}, \quad z = \tilde{Z}(\eta) - \tilde{Z}(0) < 0$$

In the model of Samelson (2022), effective stress arising from the mass-weighted mean is parameterized by a classical mixing-length eddy viscosity, extended to include a wave-effect parameter that modifies the von Kármán constant (as is done for stability effects in Monin-Obukhov similarity theory):

$$\tau = -\rho_o A_v \frac{d\mathbf{U}}{dz}, \quad A_v(z;U_{10N}) = \phi_w(U_{10N})\,\kappa\, u_*[z_{0o}(U_{10N}) - z]$$

A nominal calibration of the roughness length and wave-effect parameters is obtained from comparisons with linear Stokes-drift:

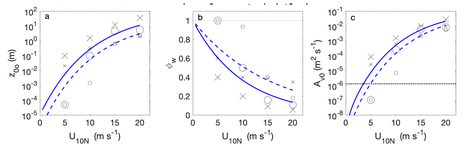

Figure from Samelson (2022).

The resulting wave-modified log-Ekman model velocity profiles that have log-layer structure for low wind speeds and linear near-surface shear for high wind speeds (Figures 2,3).

3. Model for equilibrium wind and wave drift: velocity profiles

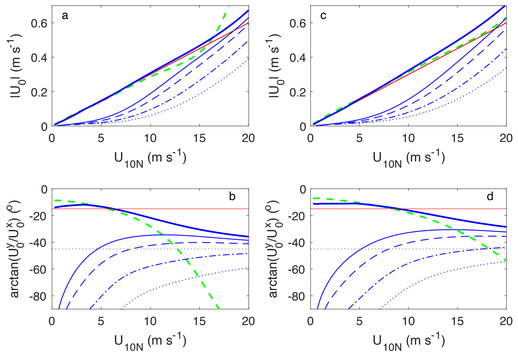

Figure 2. Model velocity vs. 10-m neutral wind speed U_{10N} for two nominal calibrations of model roughness length and wave-effect parameter. Wind-drift velocity (a),(c) magnitude and (b),(d) angle relative to surface stress, at the surface (thick blue line) and at depths of 1 m (thin), 2 m (dashed), 5 m (dashed–dotted), and 10 m (dotted), with the 3% rule-of-thumb estimate of surface drift (red). In (b) and (d), the 45° angle of the classical Ekman-layer surface velocity is shown for reference (dotted black). A log-layer estimate of surface velocity magnitude and direction is also shown (green dashed). From Samelson (2022).

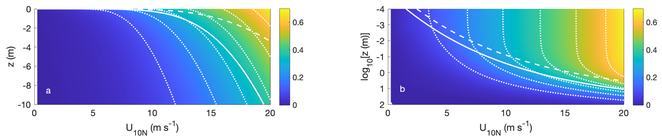

Figure 3. Magnitude of model vector velocity (m s^{-1}; shading, white contours at 0.1 m s^{-1} intervals) vs U_{10N} and (a) depth *z* or (b) base-10 logarithm of depth $\log_{10}z$ for model solutions as in Fig. 1ab. (a). The depths z_{0o} (solid white line) and $0.3z_{0o}$ (dashed white) are also shown, where z_{0o} is the wind-speed dependent roughness-length parameter. From Samelson (2022).

4. Comparison with observations

Existing observations are not adequate to provide a fully empirical calibration but initial comparisons to some existing datasets have been made (e.g., Figure 4).

Figure 4. Comparisons from Samelson (2022) of model predictions with coastal radar observations from Ardhuin et al. (2009).

(a) Observed (black line, X) and model 0 m – 1.6 m mean (blue) and 0.8 m (red dashed) velocity magnitude vs observed 10-m wind and model U_{10N}, respectively.

(b) Velocity magnitudes in (a) as percentage of corresponding wind speed.

(c) Angles of velocities in (a) relative to wind direction. Observational data digitized from Fig. 6 of Ardhuin et al. (2009).

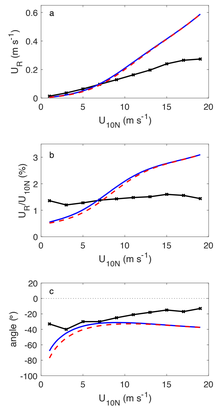

Ardhuin, F., L. Marié, N. Rascle, P. Forget, and A. Roland, 2009: Observation and estimation of Lagrangian, Stokes, and Eulerian currents induced by wind and waves at the sea surface. J. Phys. Oceanogr., 39 (11), 2820–2838.

5. Planned approach

1. Compute global (extra-equatorial) properties of sub-inertial wind-drift currents predicted by the equilibrium wind-drift model:
   - MERRA-2 reanalysis and QuikSCAT scatterometer winds
   - surface (air-sea interface) current at 0 m depth
   - surface current from mean over the upper meter or few meters of the water column.
   - statistics of spatial-derivative quantities (vertical component of vorticity; horizontal divergence and strain)
   - relation between spatial gradients in predicted wind-drift and departures from local wind-wave equilibrium?
   - implications for the associated Doppler scatterometer sampling problem
2. Examine the role of sub-inertial wind-drift currents in ocean-atmosphere interaction in coupled numerical simulations of the northern California Current System, including:
   - predicted wind-drift vs. resolved numerical-model velocity
   - kinetic energy balance of surface boundary layer
3. Refine wind-drift model through further comparison with existing observations:
   - surface drifters (undrogued SVP, CODE, CARTHE….)
   - winds from MERRA-2, QuikSCAT
   - geostrophic velocity from AVISO altimeter SSH